CRREL
REPORT 81-19

Ground-truth observations of ice-covered North Slope lakes imaged by radar

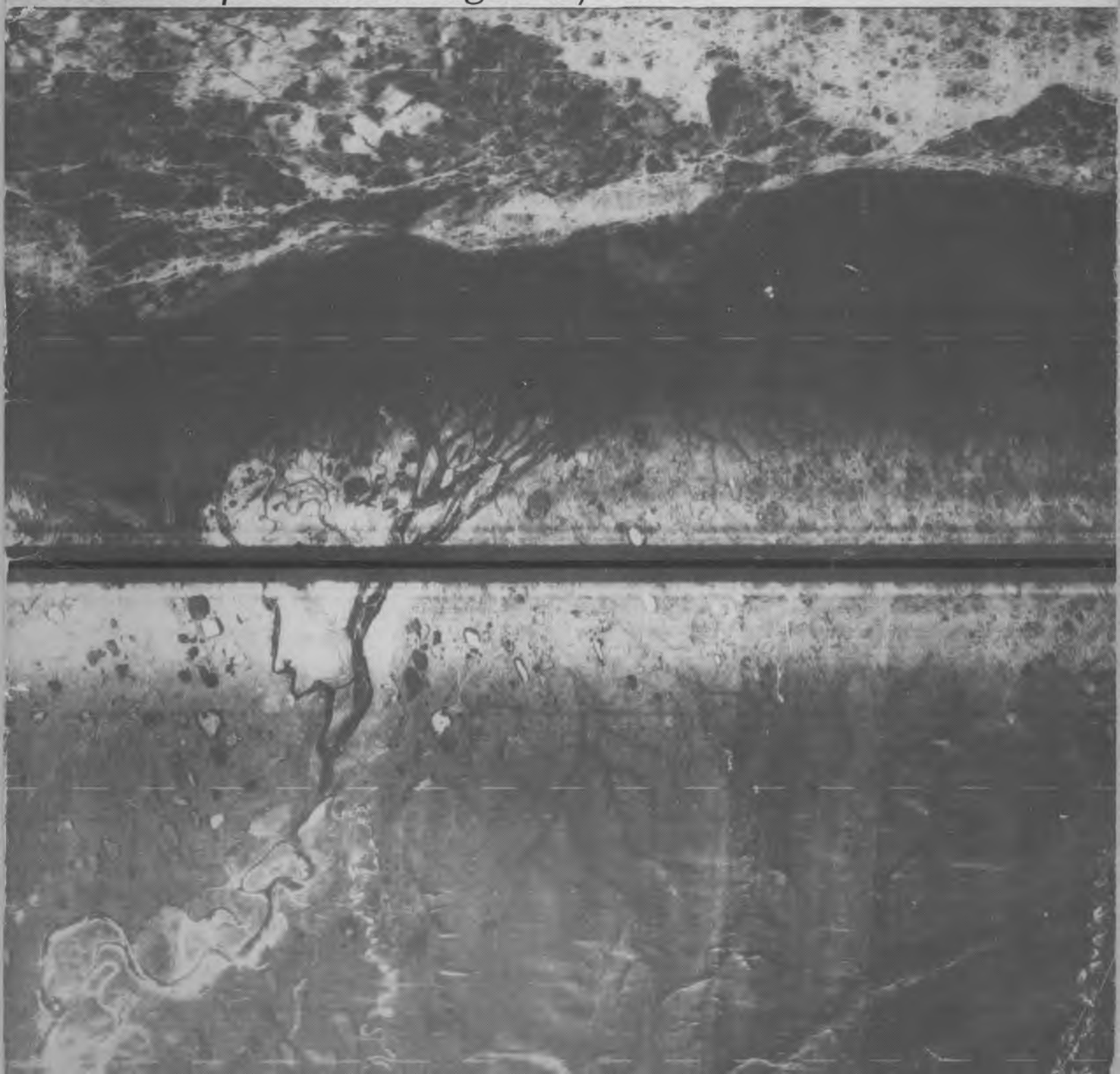

CRREL Report 81-19

Ground-truth observations of ice-covered North Slope lakes imaged by radar

W.F. Weeks, A.J. Gow and R.J. Schertler

October 1981

Prepared for
OCEAN PROCESSES BRANCH
NATIONAL AERONAUTICS AND SPACE ADMINISTRATION
By
UNITED STATES ARMY CORPS OF ENGINEERS
COLD REGIONS RESEARCH AND ENGINEERING LABORATORY
HANOVER, NEW HAMPSHIRE

REPORT DOCUMENTATION PAGE

READ INSTRUCTIONS BEFORE COMPLETING FORM

1. REPORT NUMBER: CRREL Report 81-19
2. GOVT ACCESSION NO.:
3. RECIPIENT'S CATALOG NUMBER:

4. TITLE (and Subtitle): GROUND-TRUTH OBSERVATIONS OF ICE-COVERED NORTH SLOPE LAKES IMAGED BY RADAR
5. TYPE OF REPORT & PERIOD COVERED:
6. PERFORMING ORG. REPORT NUMBER:

7. AUTHOR(s): W.F. Weeks, A.J. Gow and R.J. Schertler
8. CONTRACT OR GRANT NUMBER(s):

9. PERFORMING ORGANIZATION NAME AND ADDRESS: U.S. Army Cold Regions Research and Engineering Laboratory, Hanover, New Hampshire 03755
10. PROGRAM ELEMENT, PROJECT, TASK AREA & WORK UNIT NUMBERS:

11. CONTROLLING OFFICE NAME AND ADDRESS: Oceanic Processes Branch, NASA Headquarters, Washington, D.C. 20546
12. REPORT DATE: October 1981
13. NUMBER OF PAGES: 20

14. MONITORING AGENCY NAME & ADDRESS (if different from Controlling Office):
15. SECURITY CLASS. (of this report): Unclassified
15a. DECLASSIFICATION/DOWNGRADING SCHEDULE:

16. DISTRIBUTION STATEMENT (of this Report)

Approved for public release; distribution unlimited.

17. DISTRIBUTION STATEMENT (of the abstract entered in Block 20, if different from Report)

18. SUPPLEMENTARY NOTES

This study was performed in cooperation with the NASA Lewis Research Center, Cleveland, Ohio.

19. KEY WORDS (Continue on reverse side if necessary and identify by block number)

Alaska	Lakes
Cold regions	Radar
Ice	Water supplies

20. ABSTRACT (Continue on reverse side if necessary and identify by block number)

Field observations support the interpretation that differences in the strength of radar returns from the ice covers of lakes on the North Slope of Alaska can be used to determine where the lake is frozen completely to the bottom. An ice/frozen soil interface is indicated by a weak return and an ice/water interface by a strong return. The immediate value of this result is that SLAR (side-looking airborne radar) imagery can now be used to prepare maps of large areas of the North Slope showing where the lakes are shallower or deeper than 1.7 m (the approximate draft of the lake ice at the time of the SLAR flights). The bathymetry of these shallow lakes is largely unknown and is not obvious from their sizes or outlines. Such information could be very useful, for example in finding suitable year-round water supplies.

PREFACE

This report was prepared by Dr. W.F. Weeks and Dr. A.J. Gow of the Snow and Ice Branch, Research Division, U.S. Army Cold Regions Research and Engineering Laboratory and by R.J. Schertler of the NASA Lewis Research Center. The study was conducted for the Oceanic Processes Branch, NASA Headquarters, Washington, D.C.

The authors express their appreciation to R. Gedney and the engineering and operations staff of the NASA Lewis C-131 aircraft for making the collection of these data possible. They also thank the Navy Arctic Research Laboratory for providing air transportation to the lakes.

CONTENTS

ILLUSTRATIONS

TABLES

GROUND-TRUTH OBSERVATIONS OF ICE-COVERED NORTH SLOPE LAKES IMAGED BY RADAR

W.F. Weeks, A.J. Gow and R.J. Schertler

INTRODUCTION

In a recent series of papers (Sellmann et al. 1975, Elachi et al. 1976, Weeks et al. 1977, 1978) attention has been called to the fact that the radar returns from ice-covered lakes with apparently similar upper ice surfaces show wide variations. The patterns of these variations support the hypothesis that the areas of low return correspond to regions where the ice is thick enough to be frozen completely to the lake bottom, resulting in an ice/frozen soil interface. Conversely, where a high return is observed the ice cover is presumed not to extend completely to the lake bottom, resulting in an ice/water interface.

The hypothesis is reasonable, as ice and frozen soil have nearly the same dielectric constants (a low contrast, low return interface), while ice and water have very different dielectric constants (a high contrast, high return interface). In fact, at normal incidence the reflection coefficient at X-band frequencies is higher by a factor of about 12 for an ice/water interface than it is for an ice/frozen soil interface. The differences between the reflection coefficients of these two types of interfaces could possibly be the complete explanation if the radar beam was perpendicular to the ice/water interface. As the radar beam actually encounters the ice at angles that are appreciably different from zero, other factors must also be involved, inasmuch as the bottom of undeformed lake ice is commonly a very flat, specular surface. This is particularly true for the thick, undeformed ice covers that develop on the lakes of the North Slope of Alaska. Therefore, the return from such a smooth ice/water surface would be away from the receiver and the region would appear as a low return in the SLAR image, even if a high return surface was present (a situation similar to the low radar return observed from a calm sea). Clearly, for a strong return to reach the receiver in the aircraft additional scattering elements are required.

It has been suggested (Weeks et al. 1978) that the necessary volume scattering within the ice is the result of the numerous highly elongated cylindrical air bubbles that commonly occur in the ice on such lakes. Because the bubbles are elongated in the direction of heat flow (ice growth), the elongation in an undeformed ice cover is exactly orthogonal to both the upper and lower ice surfaces. Accordingly, the bubbles act as forward scatterers; the incoming radar pulse is only scattered downward and the outgoing radar

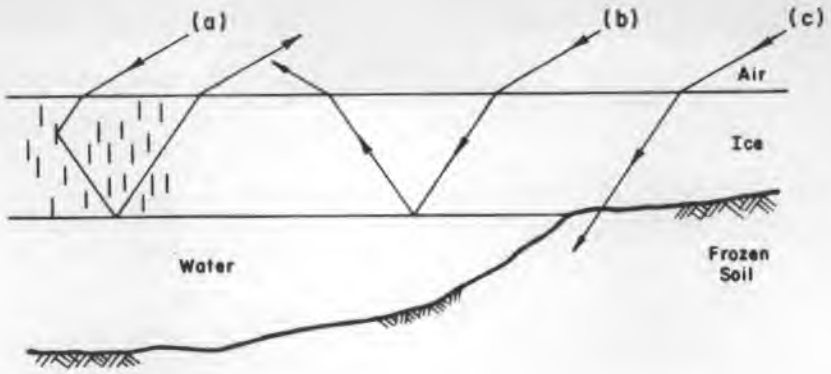

Figure 1. Schematic drawings showing the nature of the radar scattering in a) lake ice with elongated bubbles, b) bubble-free lake ice, and c) lake ice that is frozen to the bottom.

pulse (after being reflected at the ice/water interface) is only scattered upward. Therefore, for a strong radar return both the elongated bubbles and a planar ice/water interface are required, while a weak return can result from either a lack of bubbles or an ice/frozen soil interface. If the bubbles in the ice were spherical isotropic scatterers, the characteristics of the lower ice interface would be less important in controlling the strength of the radar return. Figure 1 presents schematic representations of these different situations.

Field checks of these hypotheses are limited. In the one series of such observations that has been published (Weeks et al. 1978) six sites were visited and good agreement was found between the observed ice conditions and the nature of the radar returns.

In the present paper we discuss additional ground-truth observations made at a number of lake ice sites on the North Slope, south of Lonely, Alaska, and compare them with the nature of the radar returns. We also utilize a new set of SLAR images to prepare maps showing areas of the commonly shallow North Slope lakes where water depths are greater than 1.7 m (the approximate draft of the ice cover at the time the radar images were obtained).

THE EXPERIMENT

During March 1979 the NASA Lewis Research Center C-131 aircraft flew a series of missions to study the radar returns from sea ice in the Beaufort Sea. On the way to and from the sea ice areas it was possible to obtain additional radar imagery of a portion of the North Slope of Alaska that is covered by a myriad of shallow lakes. As part of this area was included in some of the earlier SLAR studies (Sellmann et al. 1975, Weeks et al. 1977, 1978) comparisons could also be made with previous imagery. The general study area and the SLAR coverage are shown in Figure 2. The specific SLAR missions utilized were flown on 16 and 20 March 1979. The quality of the SLAR imagery was appreciably better than that of earlier investigations. The characteristics of the SLAR system used are given in Table 1. The team undertaking the ground-truth observations (Gow and Weeks) was provided with high quality SLAR images before the field sampling was undertaken. In retrospect we believe that the availability of imagery during the field observations was essential to the successful selection of suitable field test sites.

The ground-truth observations were made on 29 and 30 March 1979, approximately two weeks after the SLAR imagery was obtained. As the weather during the intervening period had been relatively stable (clear and cold), there was no reason to expect appreciable differences in the nature of the ice cover except for a few centimeters of additional ice growth.

Initially we planned to base the sampling out of Lonely, traveling back and forth to the lakes with a snowmobile. Fortunately, at the last minute we were able to arrange air transportation directly from Barrow to the sample sites. We mention this as we are now of the opinion that it would have proved most difficult, even with good maps and excellent visibility, to locate oneself precisely on the North Slope at this time of year. The terrain is extremely flat, with few

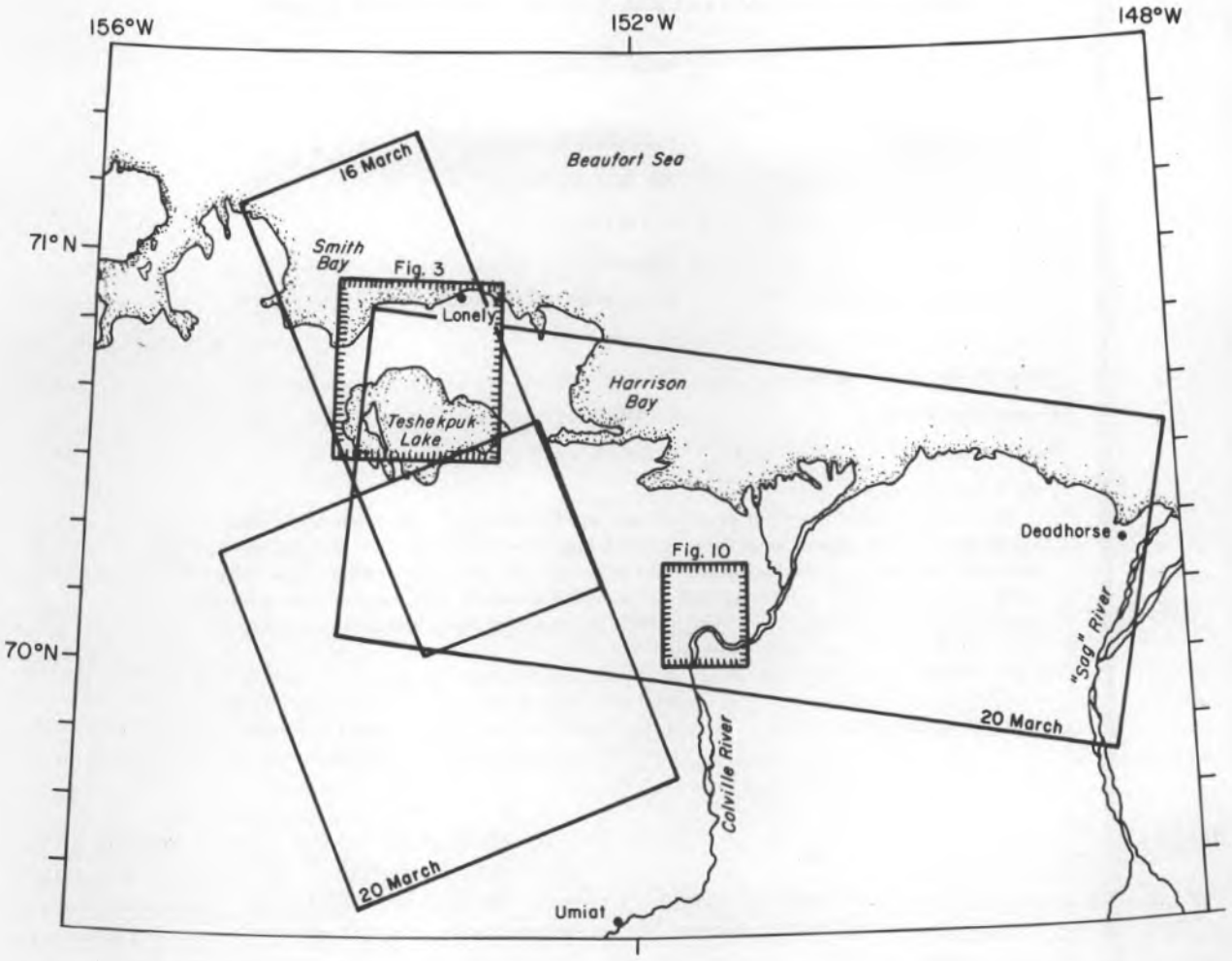

Figure 2. Part of the North Slope of Alaska showing the area covered by the SLAR imagery and the locations of the maps in Figures 3 and 10.

distinctive features, and, in addition, the entire surface was covered with snow. During the two days that we spent collecting samples, visibility was excellent, and low sun angles helped to reveal slight differences in surface topography. However, we were commonly forced to circle a prospective site several times until we could identify enough features to fix our position. Once we had landed, accurate positioning usually was impossible.

Our ground-truth studies of the lake ice focused mainly on investigations of the basic physical properties of the ice. These studies, made on samples obtained with a CRREL (7.6 cm) coring auger, included measurements of density, electrolytic conductivity, and bubble and crystal structure. Coring also yielded data on ice sheet thicknesses and provided access to the water and/or soil underlying the lake ice covers.

Table 1. Characteristics of side-looking airborne radar system.

Type	Motorola AN/APS-94D Real Aperture
Frequency	X-Band, Tunable 9.10–9.40 GHz
Polarization	Horizontal-Horizontal
Pulse width	200 nanoseconds
Output power	45 kW peak
Pulse repetition	750/second
3-dB antenna beam width	0.45 degree = 7.85 mrad
Range resolution	30 meters
Minimum detectable signal	-97 dBM
Receiver bandwidth	4.5 MHz
Swath width	50 km each side of aircraft
Digital data processing	Returns from transmitted pulses are divided into 3200 equal right antenna and 3200 equal left antenna ground range bins. For each range bin, the SLAR video signal is sampled and digitized into a six-bit data word. The digitized SLAR video data from a single radar impulse are accumulated in memory and averaged exponentially with the return from the previous pulses. Auxiliary data, including aircraft drift, ground speed and location, are multiplexed with the average radar video data.
Image outputs	Real time, full resolution, analog wet-processed film Real time, digital dry, silver-process paper or film
Digital tape output	Instrumentation tape recorder in Bi-Ø-L format, computer-compatible tape in NRZ format.

RESULTS

Figure 3 is a map showing the exact locations of the 11 different sites sampled in 1979 (sites 9-1 to 9-11), as well as 3 of the 6 sites sampled in 1976 (sites 6-A to 6-C). Figure 4 shows the radar imagery of the same area. Table 2 gives the ground-truth results for the 1979 sites and all of the 1976 sites. Also indicated is the nature of the radar return at the site in question (strong or weak). The ice porosity n was determined according to the simple relation $n = (\varrho_i - \varrho_s)/\varrho_i$, where ϱ_i and ϱ_s are the densities of pure bubble-free ice and of the ice sample, respectively, measured at the same temperature. The electrolytic conductivity of the ice, which measures the bulk content of dissolved ions, was determined on melted samples at 25°C, while the conductivity of the water under the ice was measured at ambient conditions (water temperature ≈ 0°C).

An examination of Table 2 and Figures 3 and 4 shows that of the 17 sites sampled, 8 gave weak radar returns and 9 gave strong returns. All sites with weak returns showed no water under the ice (an ice/soil interface), while at all sites with a strong return an ice/water interface was present. There were no exceptions. These observations strongly support the explanation that the difference in the strength of the return is associated with the degree of dielectric contrast at the ice/water (high contrast) or ice/frozen soil (low contrast) interface. Also, the patterns of the weak return areas correspond well with areas where the lakes would be expected to be shallow, resulting in an ice cover that is frozen to the bottom. Examples of this are 1) the dark bands around the edges of all the lakes where shallow water has to occur, 2) the dark band separating the two segments of Naluakruk Lake (Site 6-B), which is the former land between the two lake segments before they joined, and 3) the long dark septum extending into Teshekpuk Lake, just to the west of Site 9-9, which also represents a submerged boundary between two former lakes that are now joined. It was initially intended that Site 9-9 be located on the septum. However, the aircraft landed too far to the east, a fact verified on take-off when both the sample site and the lake outline were visible. The fact that the water layer under the ice at Site 9-9 was only 0.34 m thick is also interesting, as Teshekpuk is the deepest lake on the North Slope and Site 9-9 is well away (2.8 km) from the nearest land. It supports the interpretation that the dark, low-return

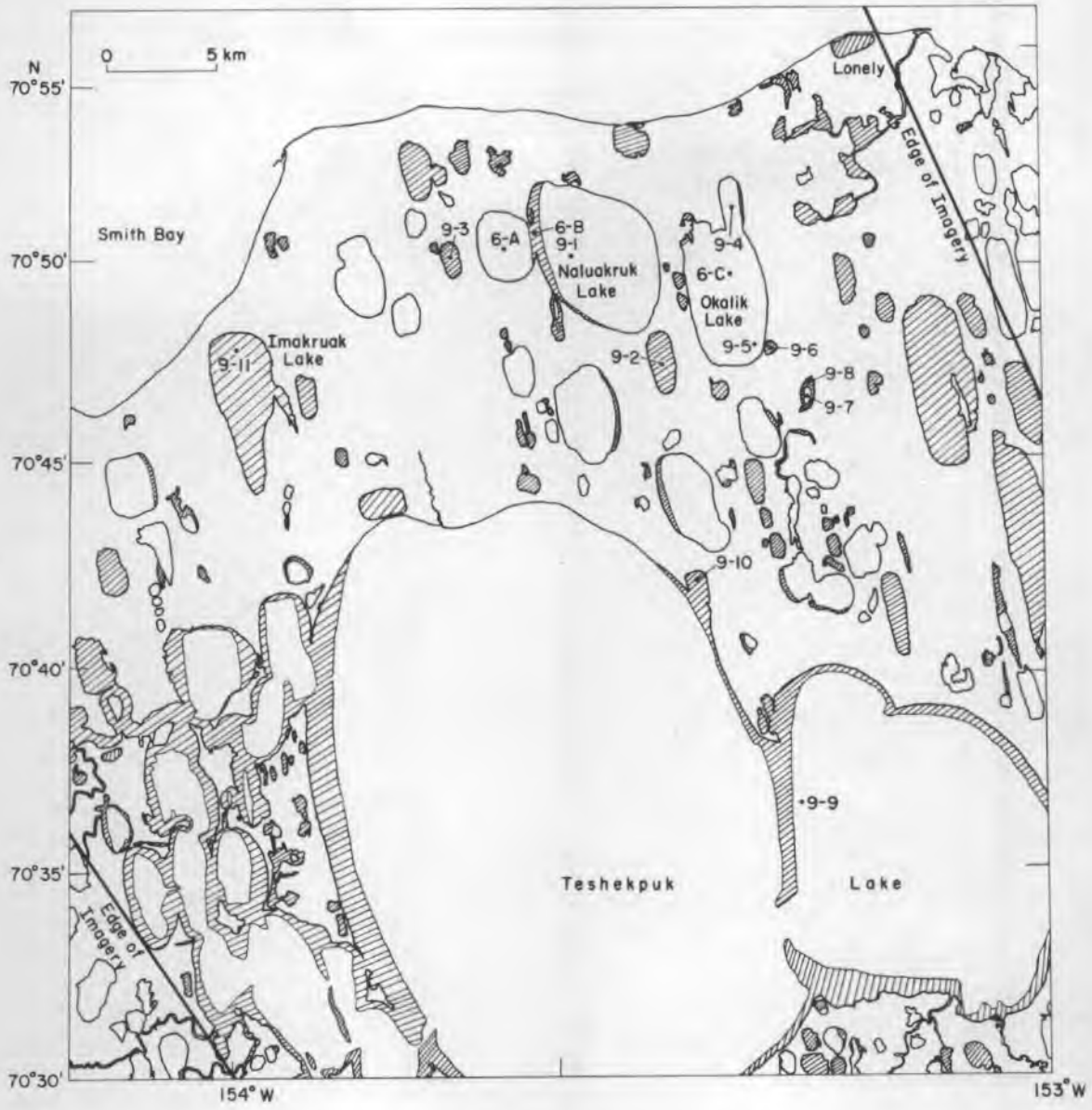

Figure 3. Map giving the exact location of the 11 sites sampled in 1979 (sites 9-1 to 9-11) and three of the sites sampled in 1976 (sites 6-A to 6-C). Also indicated is the nature of the radar returns at the different lakes (see also Figure 4). Lined lake areas are regions of weak returns (depths <1.7 m); unlined lake areas indicate strong returns (depths >1.7 m). Inspection of the base maps used to prepare this figure (U.S. Geological Survey Maps Teshekpuk C-1, C-2, D-1, D-2 [1:63,360]) will show numerous small lakes and ponds not indicated in the figure. These all showed weak radar returns.

septum indicates a region where the lake is even shallower and the ice is completely frozen to the bottom.

The other component of the present explanation of the varied radar returns from lakes with apparently similar ice (as viewed from above) is that the elongated bubbles in the ice give the volume scattering necessary for a part of the radar pulse to return to the receiver. Were such bubbles present in the ice during the late winter of 1979? Figure 5 presents photographs taken in transmitted light of 5-mm-thick vertical sections of ice from several of the sampling sites. These core sections measured 7.6 cm in diameter. Bubbles are invariably strongly elongated in the vertical. As is obvious, highly elongated (length/diameter ratios >25) bubbles are common. The bubble diameters are suprisingly constant at a

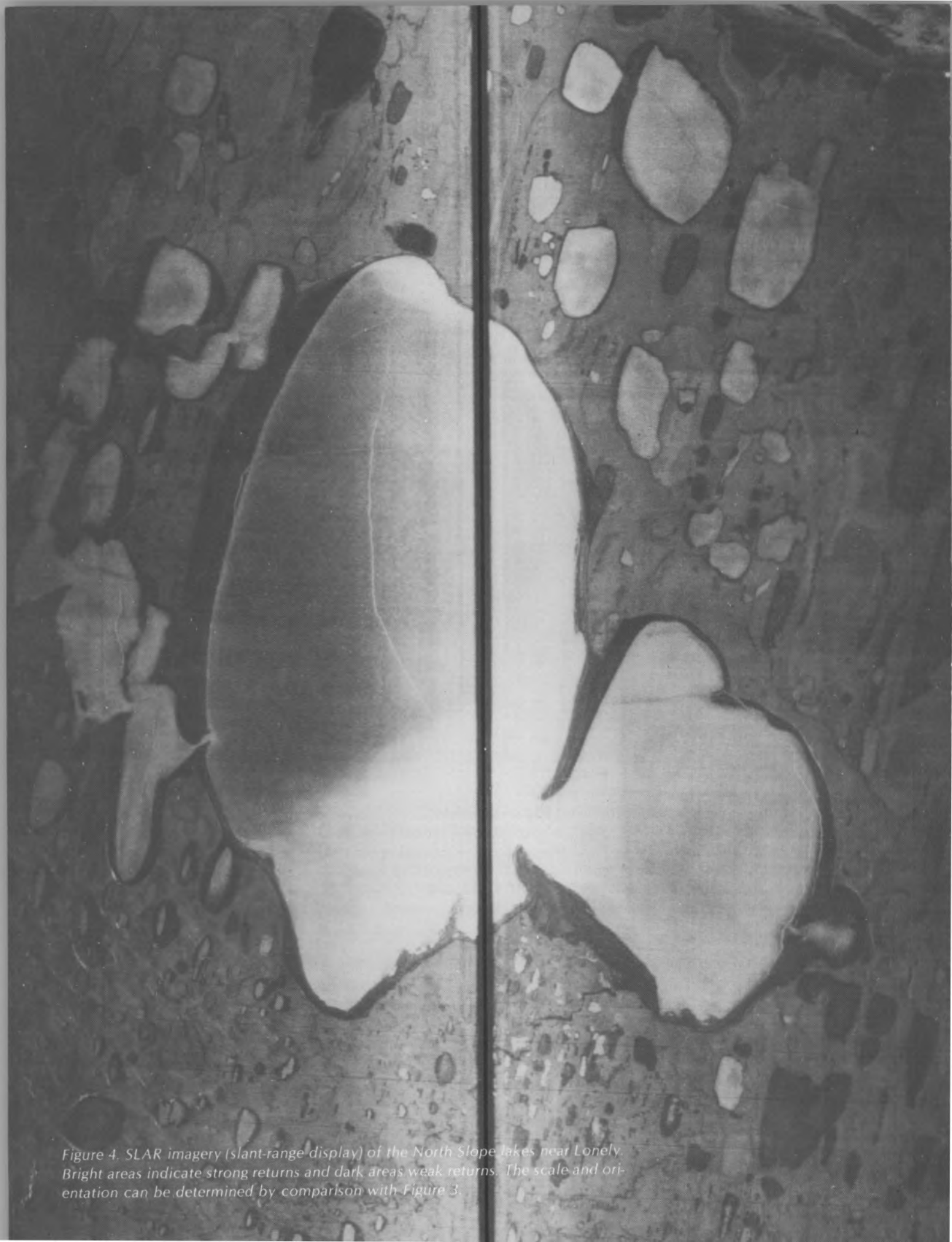

Figure 4. SLAR imagery (slant-range display) of the North Slope lakes near Lonely. Bright areas indicate strong returns and dark areas weak returns. The scale and orientation can be determined by comparison with Figure 3.

Table 2. Ground truth observations from lake ice sites shown in Figure 3.

Site no.	Nature of radar return	Thickness (m) Ice	Thickness (m) Water	Density sample location (m)	Ice density (Mg/m^3)	Ice porosity (%)	Conductivity sample location (m)	Conductivity (25°C) ($\mu mho/cm$)
				1979 Sites				
9-1	Strong	1.88	0.77	0.13–0.21	0.918	0.0	0.14–0.21	12
				1.00–1.10	0.912	0.6	0.21–0.23	4
							1.01–1.12	10
							1.10–1.12	16
							1.59–1.61	15
							1.84–1.87	24
							water	600 (0°C)
9-2	Weak	0.76	0	0.00–0.09	0.918	0.0	0.00–0.09	13
				0.30–0.48	0.885	3.6	0.09–0.11	19
				0.67–0.75	0.877	4.5	0.39–0.48	25
							0.48–0.50	16
							0.65–0.67	335
							0.67–0.74	540
							0.75–0.76	847
9-3	Weak	1.11	0	0.14–0.22	0.902	1.7	0.15–0.22	11
				0.26–0.44	0.915	0.3	0.22–0.26	19
				0.88–1.00	0.917	1.2	0.26–0.34	27
							0.34–0.43	23
							0.44–0.48	35
							0.88–0.99	43
							1.04–1.08	432
9-4	Strong	1.93	0.37	0.84–0.96	0.916	0.2	0.19–0.25	12
				1.58–1.70	0.904	1.5	0.26–0.28	42
							0.82–0.84	32
							0.84–0.89	25
							0.89–0.95	31
							0.96–0.98	18
							1.23–1.25	9
							1.58–1.69	19
							1.70–1.72	10
							water	1350 (0°C)
9-5	Strong	1.93	0.57	0.14–0.26	0.918	0.0	0.14–0.26	19
				1.07–1.20	0.893	2.7	0.26–0.28	5
				1.73–1.90	0.902	1.7	1.05–1.07	6
							1.07–1.20	5
							1.73–1.75	27
							1.90–1.94	25
							water	500 (0°C)
9-6	Weak	1.67	0	0.16–0.28	0.918	0.0	0.14–0.16	20
				0.76–0.82	0.889	3.2	0.17–0.22	6
				1.06–1.15	0.911	0.8	0.22–0.28	22
				1.50–1.65	0.915	0.3	0.82–0.84	25
							1.06–1.15	12
							1.15–1.18	10
							1.50–1.57	16
							1.57–1.64	140
							1.65–1.67	237

Table 2. Ground truth observations from lake ice sites shown in Figure 3 (cont'd).

Site no.	Nature of radar return	Thickness (m) Ice	Thickness (m) Water	Density sample location (m)	Ice density (Mg/m^3)	Ice porosity (%)	Conductivity sample location (m)	Conductivity (25°C) (μmho/cm)
				1979 Sites (cont'd)				
9-7	Strong	1.92	0.36	0.19–0.33	0.918	0.0	0.19–0.26	16
				0.83–0.96	0.912	0.6	0.26–0.33	29
				1.16–1.27	0.889	3.2	0.33–0.36	20
				1.68–1.83	0.906	1.3	0.80–0.83	44
							0.83–0.90	8
							0.90–0.96	30
							1.14–1.16	9
							1.16–1.22	7
							1.22–1.27	32
							1.68–1.75	91
							1.75–1.82	37
							1.83–1.85	62
							water	1820 (0°C)
9-8	Weak	1.70	0				water	2600 (0°C)
9-9	Strong	1.70	0.34	0.13–0.27	0.915	0.3	0.11–0.13	3
				0.98–1.10	0.876	4.6	0.14–0.20	14
				1.48–1.57	0.898	2.2	0.20–0.27	21
							0.96–0.98	5
							0.99–1.05	9
							1.05–1.10	30
							1.48–1.56	12
							1.57–1.59	7
							water	30 (0°C)
9-10	Weak	0.42	0	0.38–0.42	0.916	0.2	0.00–0.03	23
							0.03–0.05	6
							0.27–0.35	22
							0.35–0.38	25
9-11	Weak	0.15	0	0.00–0.13	0.894	2.6	0.00–0.12	1998
							0.13–0.15	3740
				1976 Sites				
								Water salinity (‰)
6-A	Strong	2.29	0.10					0.153
6-B	Weak	2.21	0					
6-C	Strong	2.31	0.58					0.163
6-D	Strong	2.34	0.66					0.716
6-E	Weak	0.71	0					
6-F	Strong	2.29	0.07					0.406

given site. Although bubble terminations are not rare, they do not appear to be as common as in lake ice from more temperate regions. That this should be the case is reasonable as the ice on North Slope lakes undergoes fewer fluctuations in growth rate during its formation than does lake ice in more temperate regions. Note that the porosity of the ice caused by the bubbles (Table 2) is at the most 4.6% and is usually less than 3%. Note also that at a number of sites the porosity of the near-surface ice was close to zero. These measurements are supported by the field observation that in general the near-surface ice contained few if any air bubbles. Apparently

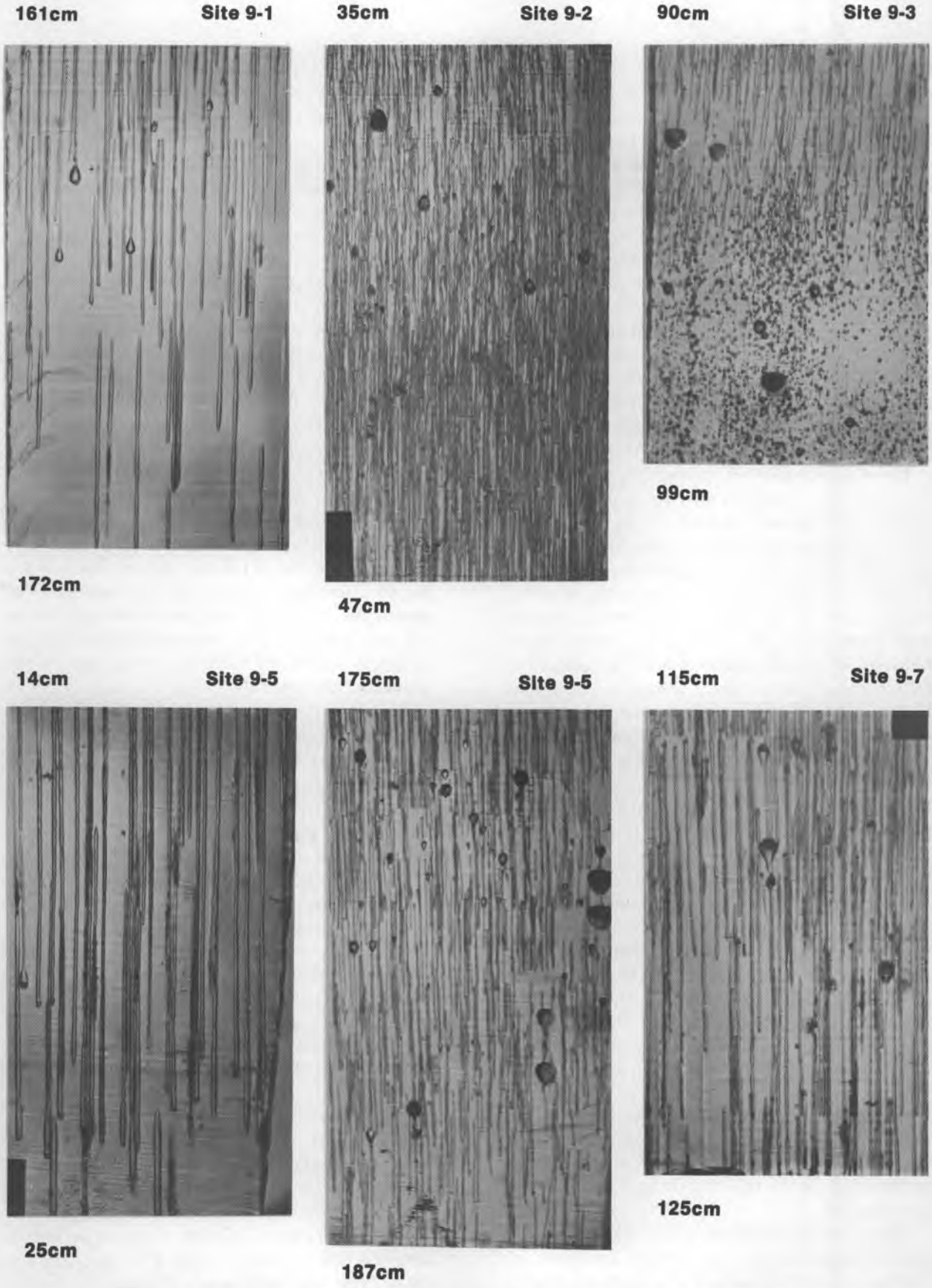

Figure 5. Photographs (transmitted light) of 5-mm-thick sections of lake ice from a number of the sampling sites. Depth intervals are as indicated.

an appreciable thickness of lake ice must form before the water below the lower ice surface becomes sufficiently supersaturated with gas to cause bubbles to nucleate. We suggest that the extremely dark areas that bound the edges of a number of the low-return lakes (for instance the lake containing Site 9-2) are produced by near-bubble-free lake ice freezing to the bottom, and that the slightly higher returns from the center portions of such lakes are caused by the direct backscatter of the radar pulses from the occasional spherical bubbles that occur, as well as from the terminations and irregularities in the cylindrical bubbles. At such locations all the forward-scattered radiation, as well as the radiation that has passed through the ice sheet without encountering a scatterer, will penetrate into the soil, resulting in a low return.

The impurity level of the majority of the lake ice is low (5 to 30 μmho/cm), corresponding to excellent quality raw water. This is in spite of the fact that the impurity levels in the lake water are generally high (measured conductivities of 500 to 1820 μmho/cm at 0°C, corresponding to salinities of 0.5 to 1.8‰). (Contrast this with a typical New Hampshire lake, with water conductivity between 40 and 60 μmho/cm and ice conductivity frequently less than 2 μmho/cm (Gow and Langston 1977.) The reason for the large differences between the ice and water compositions is that the lake ice grows with a planar ice/water interface, and the amount of impurity trapped in the ice is near that specified by the equilibrium phase relations. The exception to this is Site 9-11, where the water being frozen was sufficiently saline to cause a non-planar ice/water interface to develop, resulting in the entrapment of large amounts of impurities in the ice. The ice at this site was sufficiently saline (2‰) that a low radar return might have resulted even if an ice/water interface had been present. Another tendency apparent in a number of the conductivity profiles (Sites 9-1, -3 and -6) is the pronounced increase in conductivity as the bottom of the ice column is sampled. This is especially true at sites where the ice is frozen to the lake bed. This effect is due to the rapid increase in the impurity level of the remaining amount of residual water as the result of the rejection of impurities by the growing ice.

Other than at Site 9-11, where the ice showed the development of a sea-ice-like structure, all the ice sampled appeared to be normal congelation-type lake ice. Structural characteristics of this ice are best demonstrated in thin sections prepared with a microtome (a histological sectioning device modified to cut ice) and photographed between crossed polaroids to reveal the outlines of the crystals composing the ice. Ice at all locations was first-year ice, that is, ice produced during a single winter.

The ice texture can be described as coarsely crystalline, especially in the deeper parts of the ice sheets where the dimensions of crystals in horizontally sectioned cores frequently exceed the cross-sectional diameter of the cores (7.6 cm). In vertical sections of core the texture of the ice is typically columnar. Orientations of c-axes were measured on sections of core from several lakes in order to obtain some idea of overall fabric. Plots of c-axes (Schmidt net), together with the crystal texture photographs of ice from three lakes, are presented in Figure 6. Though most thin sections contain too few crystals for a completely adequate determination of the fabric, most nevertheless exhibit a horizontal distribution of c-axes—one of two major fabric patterns observed in lake ice sheets. Much of the ice is also characterized by the existence of distinctive subgrain structure in many of the crystals. Such features are most likely produced by stresses induced in the ice lattice during the growth of the crystals.

At Site 9-11, where the lake contains a high concentration of salts, ice with a structure and fabric closely resembling those of sea ice was formed in place of lake ice. A thin section photograph of ice from near the ice/lake bed interface at Site 9-11, together with the corresponding c-axis fabric, is presented in Figure 7.

The snow cover on top of the lakes was generally continuous, although a few scattered patches of bare ice were present (Fig. 8). Snow depths were usually 5 to 20 cm and occasional small sastrugi fields were observed. Snow densities were estimated to be in the 0.3- to 0.4-Mg/m^3 range. There was no evidence of any correlation between the nature of the snow cover or its distribution and the observed differences in radar return.

It should also be noted that there are irregular linear regions of high return on Naluakruk and Teshekpuk Lakes and to a lesser extent on Okalik Lake. Similar features were noted but at slightly different locations in the L-band imagery discussed by Weeks et al. (1978). They are definitely pressure ridges caused by the shifting of the ice cover. The high returns are attributable to the blocky nature of the ice composing the ridges. Figure 9 shows both an aerial and a surface view

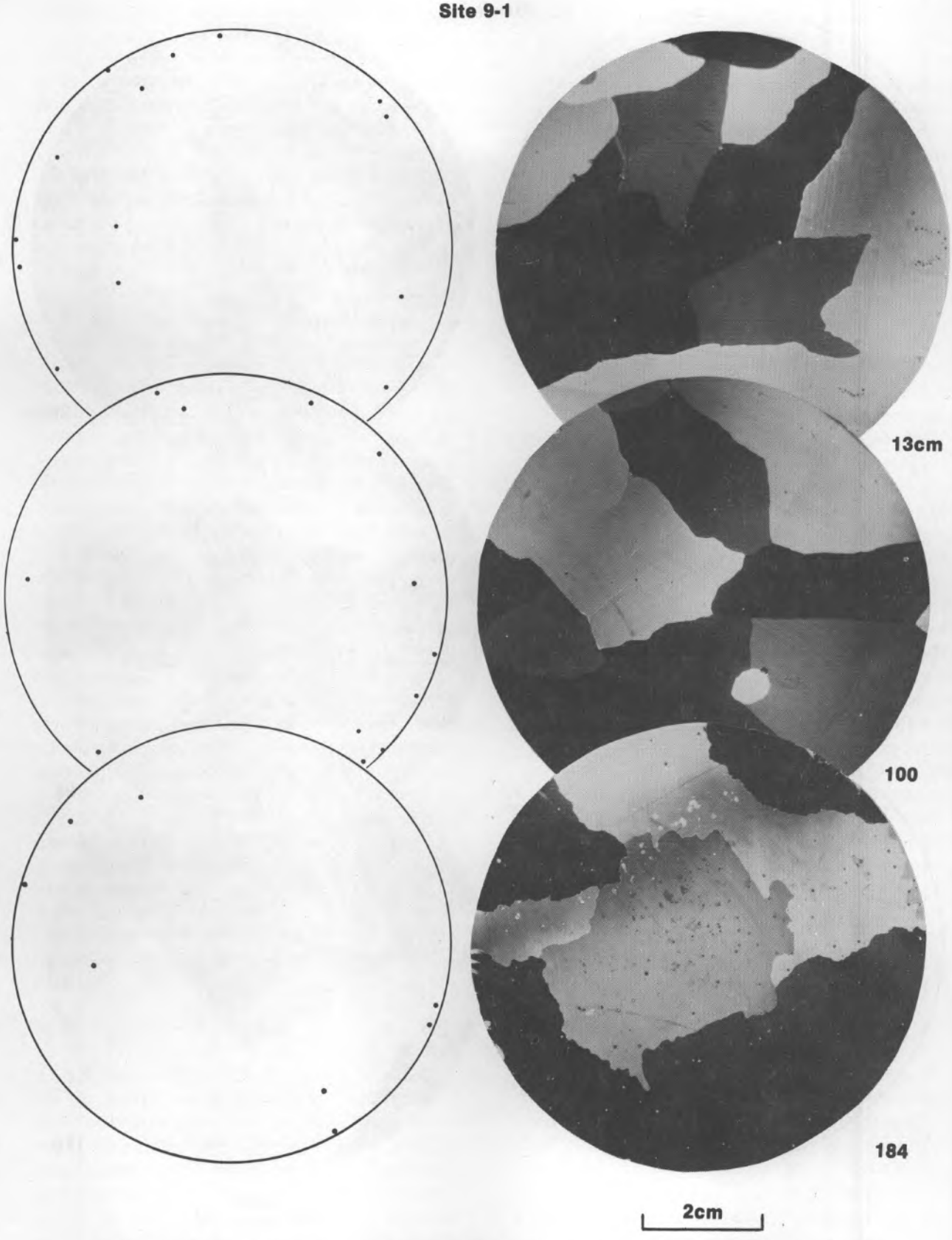

Figure 6. C-axis orientation plots (equal-area projections) and thin section photographs of ice from three of the sample sites.

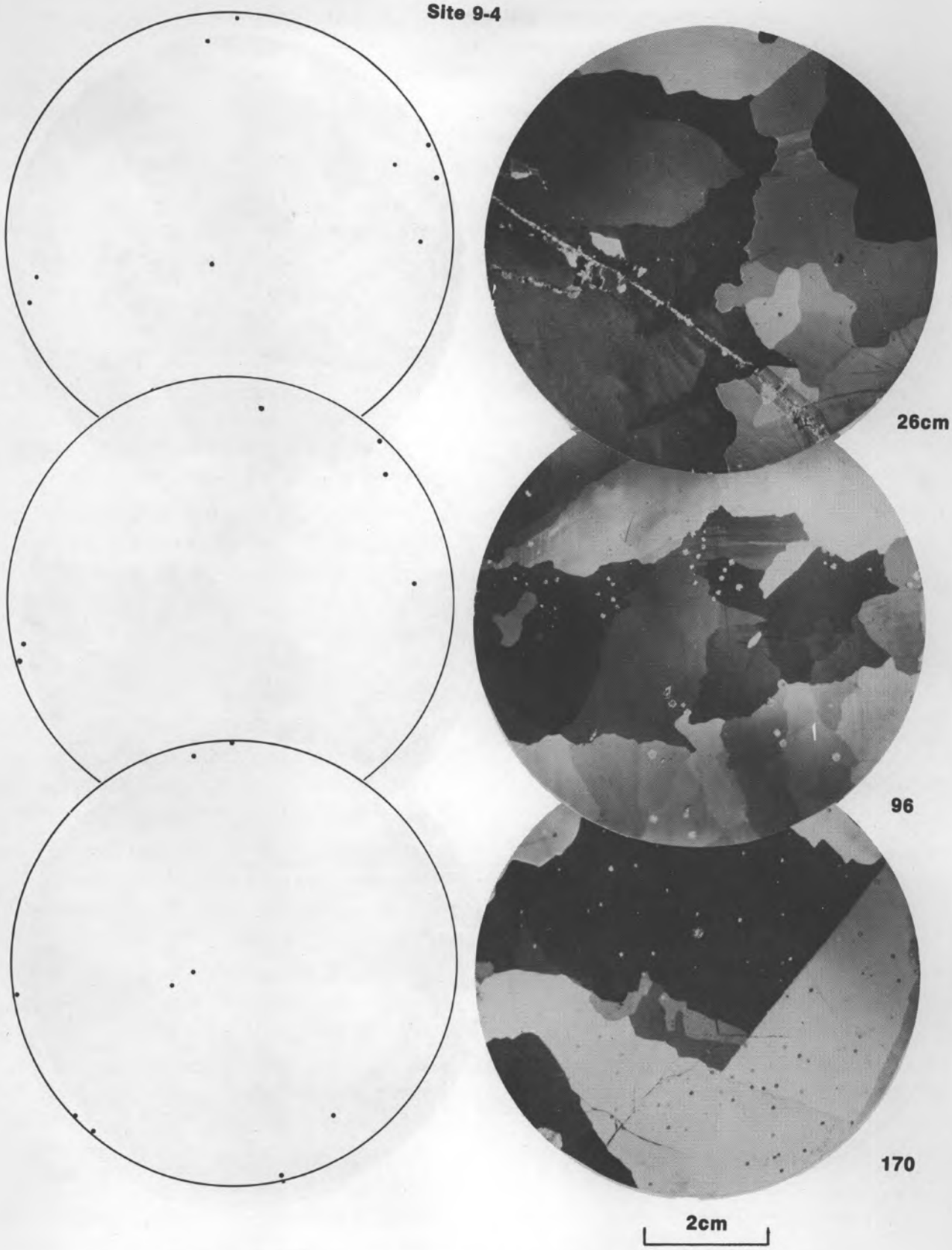

Figure 6 (cont'd). C-axis orientation plots (equal-area projections) and thin section photographs of ice from three of the sample sites.

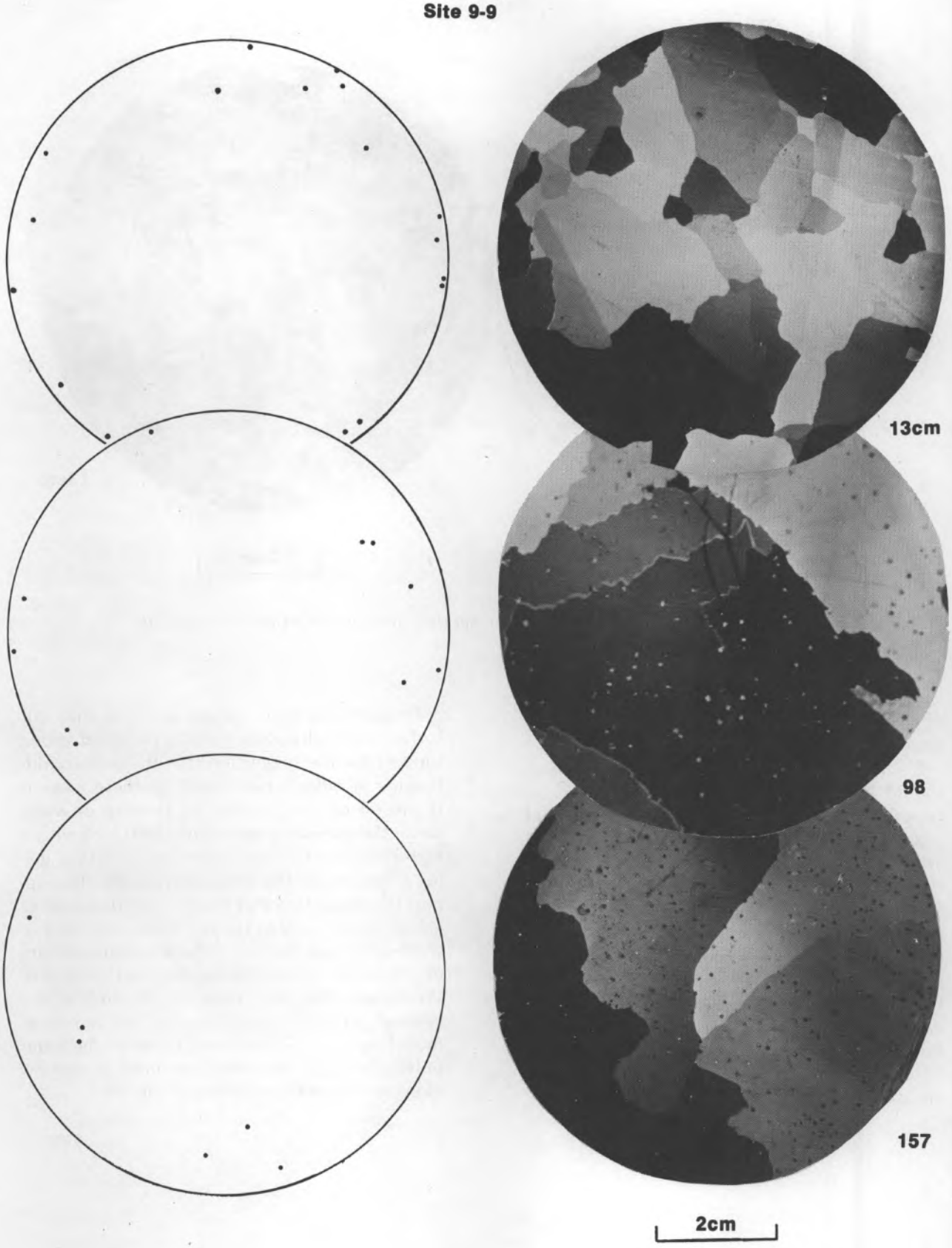

Figure 6 (cont'd).

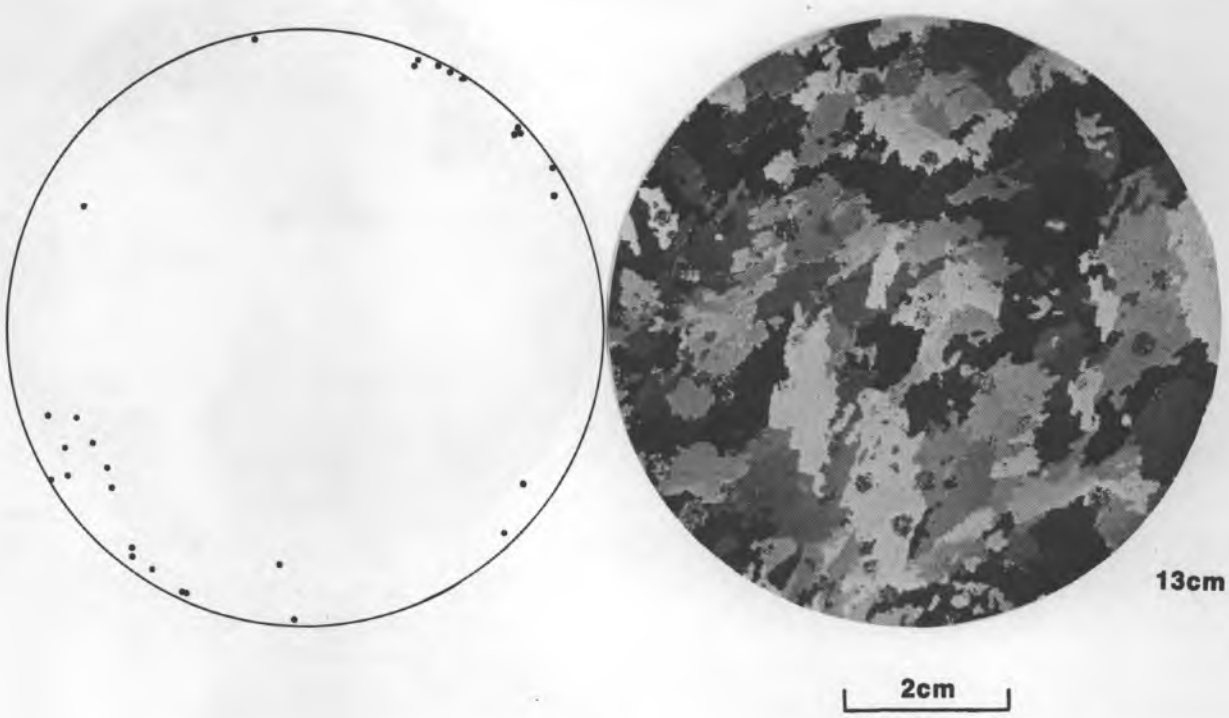

Figure 7. C-axis orientation plot and thin section photograph of the ice from Site 9-11. Note the sea-ice-like texture.

of the ridge on Teshekpuk Lake. At places the ridge was 2 m high.

Finally, one perplexing feature in the imagery should be noted. This is the lower return obtained from the western portion of Teshekpuk Lake. The dark return area has diffuse boundaries, the locations of which change with changes in the direction of the radar overpass. Similar but less pronounced lower return areas are also observed from a number of smaller lakes. Such changes in radar return do not appear to be related to the bottom topography of the lakes. We also specifically examined the nature of the snow and upper ice surface to see if we could note any features that would correlate with the low return area. There were no obvious correlations.

To summarize our results we feel that our surface-truth observations have provided strong support for the suggestion that the primary difference in radar return noted on these lakes is the result of the presence or absence of water under the ice with an ice/water interface giving a high return and an ice/frozen soil interface giving a low return. The field observations also support the suggestion that there are sufficient elongated bubbles within the ice to provide the forward scattering required if there is to be a return of the radar pulse to the receiver on the aircraft. We suggest that the next step in the study of this general problem should be the mathematical modeling of the interactions between the radar pulse, the upper and lower ice surfaces, and the elongated bubbles enclosed in the ice.

Figure 8. Two views of representative snow conditions on the sampled lakes.

Figure 9. Aerial and surface views of the pressure ridge on Teshekpuk Lake.

MAPS OF COMPLETELY FROZEN NORTH SLOPE LAKES

If our interpretation of the radar imagery is correct, then existing imagery can be used to prepare maps showing the lakes or parts of lakes that are frozen completely to the bottom. We could, of course, simply reproduce the radar images. However, they would be very large. Also, the image degradation and scale reduction associated with preparing such illustrations would result in the loss of much useful detail. Therefore, we have chosen to prepare representative maps that summarize the nature of the radar return from lakes in two different areas.

The average measured ice thickness at the time of the radar overflights was 1.88 m (range 1.70 to 1.93 m). Assuming that the ice covers are free-floating and of approximately constant thickness throughout the study area, a water depth of about 1.7 m should correspond to the boundary between regions of low and high radar return within a given lake. Figure 3 is such a map, prepared using U.S. Geological Survey (1:63,360) topographic sheets Teshekpuk C-1, C-2, D-1 and D-2 as a base. We have also prepared another example (Fig. 10) which uses the Harrison Bay A-3 topographic sheet as a base. As can be seen in Figure 2, the area covered by the Harrison Bay sheet is about 56 km southeast of the Teshekpuk Lake area. The blind areas in Figure 3 are too far to the side of the aircraft to provide good imagery (low glancing angles and poor returns). In some locations of the image used to prepare Figure 10, contrast was not adequate to allow a clear determination of the nature of the return; such lakes are marked with a question mark. In addition, the imagery in the vicinity of the Colville River (Fig. 10, lower right corner) shows many strong returns (presumably due to the presence of steep banks and gravel bars) which make the interpretation of the returns from both the river ice and from the nearby lakes rather speculative. Although we have not marked this on the map, most of the Colville gives a low return, indicating that it is frozen to the bottom. A somewhat different problem was encountered in the upper left corner of Figure 10, where the steep banks and narrowness of Judy Creek make interpretation difficult.

When the radar-return maps (Fig. 3 and 10) are compared with the original USGS topographic maps, the reader will note the actual presence of innumerable small lakes that are not indicated on the radar maps. All of these small lakes give weak radar returns, indicating they are frozen to the bottom. In using Figures 3 and 10 it should be remembered that the slant-range radar image contains geometric distortions relative to the map. In preparing the map we have attempted to remove these distortions visually. Even considering these difficulties, it is clear that the SLAR imagery and the maps prepared from the imagery

Figure 10. Map of radar returns from the lakes on the Harrison Bay (A-3) quadrangle (1:63,360). Lined lake areas are regions of weak returns (depths <1.7 m); unlined lake areas are strong returns (depths >1.7 m).

contain a great deal of useful information concerning the water depths of North Slope lakes that is not currently available, and that would be expensive to obtain by conventional means. A person interested in details about a specific location is advised to examine the original imagery (available at CRREL or at NASA Lewis).

In conclusion it should be noted that in general the lakes toward the Brooks Range (i.e. toward the south) are deeper than 1.7 m, while the lakes near the Arctic Ocean are commonly quite shallow. The imagery also indicates that lakes giving a strong return are particularly rare in the vicinity of the Prudhoe Bay oilfield. If this had been known prior to the development of the field, it would have been helpful in site planning as well as in prospecting for suitable fresh water sites.

LITERATURE CITED

Elachi, C., M.L. Bryan and W.F. Weeks (1976) Imaging radar observations of frozen arctic lakes. *Remote Sensing of Environment,* vol. 5, p. 169–175.

Gow, A.J. and D. Langston (1977) Growth history of lake ice in relation to its stratigraphic, crystalline and mechanical structure. USA Cold Regions Research and Engineering Laboratory, CRREL Report 77-1, 24 p. ADA036228.

Sellmann, P.V., W.F. Weeks and W.J. Campbell (1975) Use of side-looking airborne radar to determine lake depth on the Alaskan North Slope. CRREL Special Report 230, 6 p. ADA011249.

Weeks, W.F., P.V. Sellmann and W.J. Campbell (1977) Interesting features of radar imagery of ice-covered North Slope lakes. *Journal of Glaciology,* vol. 18, no. 78, p. 129–136.

Weeks, W.F., A.G. Fountain, M.L. Bryan and C. Elachi (1978) Differences in radar return from ice-covered North Slope lakes. *Journal of Geophysical Research,* vol. 83, no. C8, p. 4069–4073.